International Journal of Metallurgical Engineering 2013, 2(2): 137-141
DOI: 10.5923/j.ijmee.20130202.04

# Comparison between Conventional Annealing and Rapid-Transformation Annealing of Low-Carbon Steel

**A. Karmakar, D. Chakrabarti***

The Department of Metallurgical and Materials Engineering, Indian Institute of Technology (I.I.T.) Kharagpur, 721-302, Kharagpur, West Bengal, India

**Abstract** A comparative study between conventional annealing (CA) and rapid transformation annealing (RTA) of cold-rolled, low-carbon (microalloyed) steel having different starting microstructures showed that fine-ferrite grain sizes (4-6 μm) with hard-phases such as, martensite and bainite in RTA treated samples offered much higher strength (YS>800 MPa) and satisfactory elongation ($e_t$>15%) compared to the CA samples. RTA also resulted in better strain-hardening ability, absence of yield point phenomenon and comparable tensile toughness to CA.

**Keywords** Cold-Rolling, Rapid Transformation Annealing (RTA), Conventional Annealing (CA), Low-Carbon Steels

## 1. Introduction

Search of high-strength, cold-rolled and annealed steels for automotive applications are driven by the potential reduction in car-weight, improvement in fuel-efficiency and crash-resistance. Conventional annealing (CA) of low-carbon (C ≤ 0.10) steels in batch-annealing furnace using slow heating rate (<10 ℃/s) and prolonged holding (> 1 hr.) at a temperature (600-700 ℃) below $A_{c1}$ offers yield strength (YS) of 200-300 MPa[1]. Inter-critical annealing in continuous annealing furnace at ~730-830 ℃ for short holding times (< 2 min), followed by water-quenching of cold-rolled, dual-phase grades increased YS to ~300-600 MPa[2, 3]. Ultra-fine grained (grain size < 3 μm) steels developed by severe plastic deformation offered a significant rise in YS to ~800 MPa, but hampered the strain-hardening ability and uniform elongation ($e_u \leq 5\%$)[4]. TRIP and TWIP steels on the other hand, show excellent combination of strength and ductility (YS of 400-600 MPa, UTS of 700-900 MPa, $e_t$ ~ 25-40%[5], however, weldability of those high alloy grades remains an issue.

In order to improve the strength after conventional (recrystallisation) annealing different starting microstructures have been used before cold-rolling[6-8]. Due to the requirement of lesser rolling load and less chance of cracking, rolling of mixed ferrite-martensite structure is easier than that of fully hardened (i.e. martensitic) structure. Ferrite-martensite starting structure showed better tensile properties (YS of 370-470 MPa and uniform elongation, $e_u$ of 16-22%) compared to ferrite-pearlite starting structure (YS of 270-330 MPa and $e_u$ of 14-20% $e_u$)[7, 8]. Improvement of YS to ~ 470 MPa[8] was however, not to the level of strength obtained in ultra-fine grained, DP or TRIP steels[2-5].

In the present study, in search of higher strength, cold-rolled samples having different starting microstructures were subjected to rapid-transformation annealing (RTA) treatment. RTA is characterized by rapid heating (heating rate, $R_H$ = 200-300 ℃) of cold-rolled steels above $A_{c1}$, followed by short-holding (5-60 s) and rapid cooling (cooling rate, $R_C$ > 100 ℃)[9-11]. Much higher heating rate is used in RTA compared to the inter-critical annealing of DP or TRIP steels. Beneficial effect of RTA is well known[9-12], although comparative assessment between RTA and CA treatments has rarely been carried out in a systematic way and that makes the objective of the present study. Use of different starting microstructures also provided an additional opportunity for the improvement in mechanical properties and theoretical understanding of the RTA treatment.

## 2. Experimental Details

Samples from a 6 mm thick hot-rolled strip containing 0.1 C, 0.33 Si, 1.42 Mn, 0.01 P, 0.003 S, 0.035 Al and 0.007 N (all wt%) has been reheated to 1150 ℃, soaked for 30 min and subjected to three different heat-treatments, namely furnace-cooling (FC), step-quenching (SQ) and intermediate-quenching (IQ). Details of those treatments are reported in[8]. Heat-treated samples were cold-rolled to 80% reduction and were annealed either inside a muffle furnace at 600 ℃ for 1-10 hr. (CA treatment) or immersed inside a slat-bath at $T_A$ = 850 ℃ for $t_A$ = 5-60 s (RTA treatment), before water-quenching. Selection of annealing temperature

* Corresponding author:
debalay@metal.iitkgp.ernet.in (D. Chakrabarti)
Published online at http://journal.sapub.org/ijmee

($T_A$) was based on the dilatometric study carried out using BAHR®-Thermoanalyse (DIL 805A/D model) dilatometer. K-type thermocouple, which continuously monitored the sample temperature during annealing, showed a heating rate ($R_H$) of ~30 ℃/s for CA treatment and ~300 ℃/s for RTA treatment. Cross-section of the annealed strips were prepared following standard metallographic techniques and investigated by optical microscope, scanning electron microscope (SEM) and image analysis. Determination of average ferrite ($\alpha$) grain size was based on the measurement of at least 500 grains in terms of equivalent circle diameter (ECD) size. Tensile specimens have been prepared following ASTM E-8M standard and tested in an Instron-8862 Universal Testing Machine (10 ton capacity) at room temperature (25 ℃) using a cross-head velocity of 1 mm / min.

### 3.1. Microstructural Characterisation

FC, SQ and IQ heat-treatments on the as-received strip resulted in three different starting-microstructures namely, ferrite + pearlite, ferrite + blocky-martensite and ferrite + fibrous-martensite, respectively. Detailed discussion and characterization of the initial microstructure are reported earlier[8]. Microstructures of cold-rolled samples and cold-rolled and annealed samples are presented in Figure 1 and Figure 2, respectively. In case of cold-rolled ferrite + pearlite structure, increase in $R_H$ from 30 ℃/s to 300 ℃/s resulted in ~30-40 ℃ rise in $A_{c1}$ from ~750 ℃ to ~780 ℃ and $A_{c3}$ from ~905 ℃ to 930 ℃. Those values were much higher than the equilibrium transformation temperatures ($A_{e1}$ ~ 680 ℃ and $A_{e3}$ ~ 860 ℃), predicted from the Thermo-Calc® software, which is expected[13-16]. Annealing temperature for RTA ($T_A$ = 850 ℃), therefore, lies in the inter-critical temperature range.

## 3. Results and Discussion

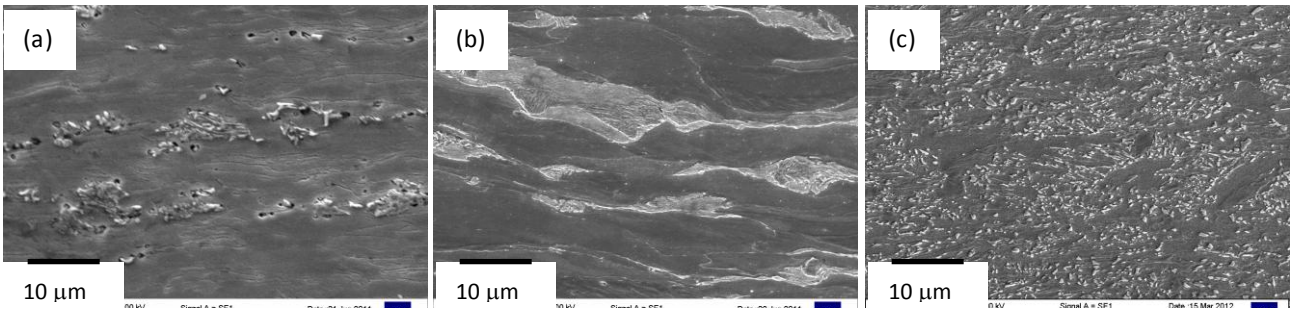


**Figure 1.** Microstructures of (a) ferrite + pearlite, (b) ferrite + blocky-martensite and (c) ferrite + fibrous-martensite samples after 80% cold-rolling

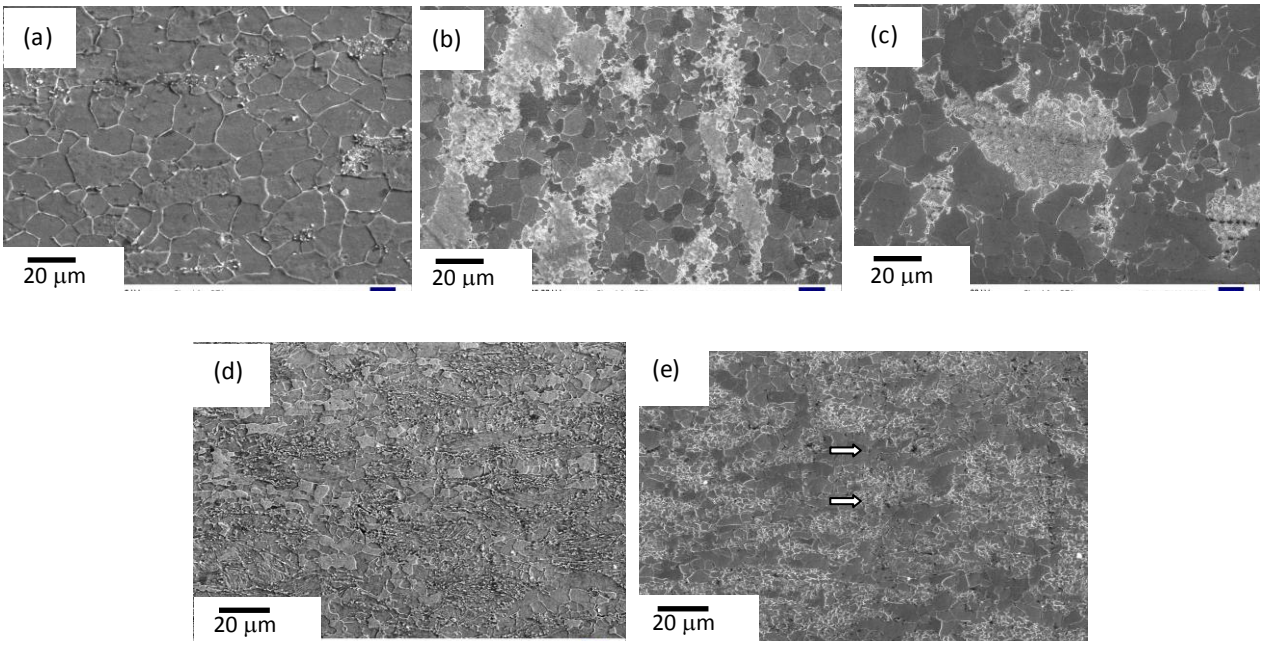


**Figure 2.** Microstructures of cold-rolled and annealed samples for different starting structures: (a) ferrite + pearlite after conventional annealing (CA) at 600 ℃ for 6 hrs. (b) ferrite + pearlite, (c) ferrite + blocky-martensite, (d) ferrite + fibrous-martensite after RTA at 850 ℃ for 5 s, and (e) ferrite + fibrous-martensite after RTA at 850 ℃ for 30 s. Coarse- and fine-grain regions in the bimodal grain structure in (e) are indicated by arrows

**Table 1.** Comparison between CA and RTA samples in terms of average ferrite grain size ($D_\alpha$) and tensile properties, for different starting microstructures

| CA | $D_\alpha$ (μm) | YS (MPa) | UTS (MPa) | $e_u$ (%) | $e_t$ (%) |
|---|---|---|---|---|---|
| Ferrite+pearlite | 14-17 | 320-356 | 368-396 | 8.1-11.3 | 26.3-28.7 |
| Ferrite+blocky-martensite | 7-9 | 382-436 | 429-463 | 18.8-21.0 | 25.5-34.4 |
| Ferrite+fibrous-martensite | 5.2-6.3 | 440-487 | 477-517 | 20.1-22.0 | 28.9-32.7 |
| RTA | | | | | |
| Ferrite+pearlite | 9-11.5 | 654-826 | 835-911 | 9.7-10.9 | 12.6-15.0 |
| Ferrite+blocky-martensite | 6-10 | 850-1080 | 1040-1269 | 8.0-10.6 | 15.7-19.7 |
| Ferrite+fibrous-martensite | 3.6-5.8 | 841-1210 | 995-1293 | 8.3-15.0 | 12.0-24.0 |

Besides bending and thinning of cementite (θ) lamellae, dislocation pile-up against the lamellae in ferrite + pearlite structure can disintegrate them upon cold-rolling, Figure 1a [17]. Cold-rolling of ferrite + blocky-martensite structure leads to heterogeneous plastic-flow with higher strain-accumulation inside the softer α-phase, Figure 1b. Due to fibrous morphology with alternate layers of α and martensite, more homogeneous plastic deformation is expected in ferrite + fibrous-martensite sample, Figure 1c. Being the supersaturated solution of C, annealing of deformed martensite results in the precipitation of finer θ-particles on the dislocation nodes, compared to that obtained after the fragmentation of pearlite in ferrite + pearlite structure[4, 6, 8, 17], Figure 2a. Lower strain-accumulation in ferrite (α) and the presence of coarser θ-particle size can explain the coarser α-grain size obtained after CA in ferrite + pearlite samples, Table 1. More uniform strain-distribution and higher stability of the θ-particles resulted in finer α-grain sizes in ferrite + fibrous-martensite samples after CA treatment, than that in ferrite + blocky martensite, Table 1. Higher stability of θ-particles in ferrite + fibrous-martensite as reported earlier[8], compared to the other structures has been attributed to the partitioning of Mn during IQ heat-treatment, resulting in Mn enrichment within the θ-particles after cold-rolling and annealing[8].

Microstructures obtained after the RTA was comprised of untransformed ferrite grains and a mixture of fine-ferrite, bainte and martensite (Figure 2(b-e)), which formed during water-quenching of austenite (γ). With the increase in annealing time ($t_A$) from 5 s to 60 s, fraction of transformed phases increased continuously from 37% to 65% in ferrite + pearlite, from 28 to 78% in ferrite + blocky-martensite and from 28 to 65% in ferrite + fibrous-martensite structure. Presence of ~35%, ~5%, ~25% unrecrystallised α-grains in ferrite + pearlite, ferrite + blocky-martensite and ferrite + fibrous-martensite structures, respectively, after 5 s annealing and nearly complete recrystallisation after 60 s annealing indicated to the interaction between α-recrystallistaion and α→γ transformation, which is a characteristic feature of the RTA treatment[9-14]. α-Recrystallisation kinetics, γ formation kinetics and the interaction between the both depend on several factors, as discussed below.

Rapid heating is expected to slow-down the non-isothermal recrystallisation kinetics of deformed α compared to the slow-heating rate[14-16]. Higher the strain-accumulation in α, faster will be the recrystallisation kinetics and lesser will be the interaction, which holds true for Ferrite+blocky-martensite. Presence of fine-microalloy precipitates, such as, Nb(C,N) and V(C,N) and fine, θ-particles, which formed during reheating of deformed martensite, can also retard the α-recrystallisation and therefore, promote the interaction to take place[9-11].

Presence of unrecrystallised α-grains, on the other hand, may encourage the strain-induced α→γ transformation[9, 10]. Kinetics of γ formation will also depend on the available ferrite-carbide interface area, which is the nucleation site for γ[9, 15]. Rapid heating prevents the spheroidization of carbides in deformed ferrite + pearlite structure, and unspheroidized carbides transform to γ at a faster rate[15], which can explain the higher γ fraction observed in ferrite + pearlite at the initial stage of annealing. As Mn diffusion is much slower than C diffusion, higher Mn enrichment inside the θ-particles in α+$M_f$[8] could have delayed the dissolution of those particles during annealing, which resulted in slower rate of austenitisation in ferrite + fibrous-martensite, with respect to ferrite + blocky-martensite. Due to the higher heating rate and small dwell time used in RTA, θ-particles did not get time to distribute uniformly throughout the microstructure, resulting in coarse blocks of γ formed by the short-range C-diffusion, covering prior-pearlite or prior-martensite regions in ferrite + pearlite and ferrite + blocky-martensite samples, respectively, Figure 2(b and c) [11, 15]. Fibrous martensite morphology in Ferrite + fibrous-martensite sample resulted in more uniform distribution of θ-particles and hence, γ islands during RTA, compared to the other starting structures, Figure 2(d and e).

Etching the RTA treated samples in hot picric-acid solution showed the presence of fine γ-grain sizes (3-8 μm), which indicated to the increased γ-nucleation during rapid-heating[9-12]. Localised austenitization in ferrite + pearlite and ferrite + blocky-martensite samples also restricted the γ grain-growth as the γ grains impinged early. In ferrite + fibrous-martensite samples γ nucleated around the fine θ-particles (distributed quite homogeneously) and eventually consumed the particles during annealing, forming small γ-islands.

In general, γ transformation under the rapid-heating is known to be governed by para-equilibrium condition, which requires the diffusion of C without the diffusion of substitutional solutes (such as, Mn and Si)[9, 13, 15, 18]. Segregation of Mn and Si at the α/γ interface increased the

hardenability of γ[9, 10, 13]. On the other hand, fine γ-grain size can reduce the hardenability. Fast-heating and short holding time could have been insufficient for the homogenization of coarse γ-blocks in terms of C, contributing to the formation of different phases (fine-ferrite, bainite and martensite) in ferrite + pearlite and ferrite + blocky-martensite structures after water-quenching[14]. Mixed (or bimodal) ferrite-grain structures has been observed in ferrite + fibrous-martensite sample, with coarse α-grains (6-10 μm) being present along with the ultra-fine α-grains (1-2 μm), Figure 2e. Ultra-fine grain regions coincided with the regions richer in martenstic islands (i.e. prior γ-islands), which prevented the α-grains to grow[18]. Therefore, RTA treatment on cold-rolled samples of different starting microstructures can produce different microstructural morphologies.

The difference in average α-grain sizes after RTA for different starting microstructures, Table 1, can be explained in view of recrystallistaion-transformation interaction and the distribution of θ-particles and hence, γ-islands. The interaction was more severe in both ferrite + pearlite and ferrite+fibrous-martensite, than that in ferrite + blocky-martensite. However, more uniform distribution of fine γ-islands in ferrite + fibrous-martensite (than that in ferrite + pearlite) resulted in finest-α grain size in ferrite + fibrous-martensite by restricting the grain growth, Table 1. Beneficial effect of rapid heating has been explored by heating a 80% cold-rolled ferrite + pearlite sample to 850 ℃ at a slow rate ($R_H$ = 1 ℃/s) and water-quenching after isothermal holding for 30 s. The α-grain size obtained after slow heating (20 μm) was nearly two-times higher than that obtained after RTA, which can be attributed to the delayed α-recrystallisation and grain-growth under rapid heating. Higher transformed fraction (50%) in RTA sample compared to the slowly heated sample (40%) was an interesting observation and is under investigated. Such a difference could have resulted from the different conditions for austenite formation: para-equilibrium under fast heating and ortho-equilibrium under slow heating.

### 3.2. Evaluation of Mechanical Properties

Typical engineering stress-strain curves of the CA and RTA samples are shown in Figure 3. As the time and temperature used in RTA and CA were entirely in different range, Hollomon-Jaffe parameter (HJ-Parameter[8]) has been used to compare their strength, Figure 4a, and ductility, Figure 4b, using the same scale along the abscissa. With respect to CA treatment, RTA offered much higher YS and UTS (~400 MPa higher) due to fine α-grain size and presence of harder phases (bainite and martensite) in the microstructure[9-12]. Taking account of the high-strength of RTA samples, average $e_u$~10% and average $e_t$~20% can be considered as satisfactory, Table 1. The scatter in mechanical properties in Figure 4(a and b) resulted from the use of different microstructures before cold-rolling. Comparing between different starting structures, the best tensile properties obtained in α+$M_f$ samples (Table 1) can be attributed to finest α-grain size along with finest θ-particle size in case of CA samples and more uniform distribution of small martensitic islands in case of RTA samples.

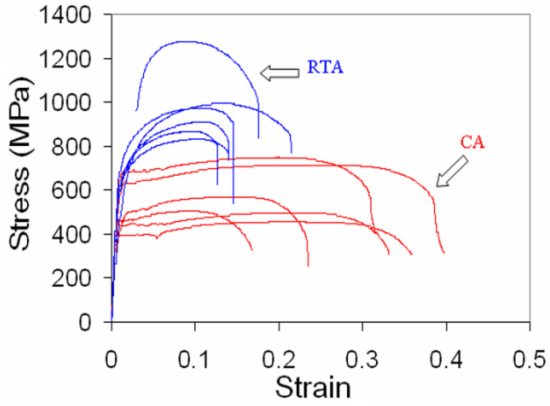


**Figure 3.** Engineering stress-strain curves of the selected CA samples (annealed at 600 ℃ for 6 hrs.) and RTA samples (annealed at 850 ℃ for 15-30 s) for different starting microstructures

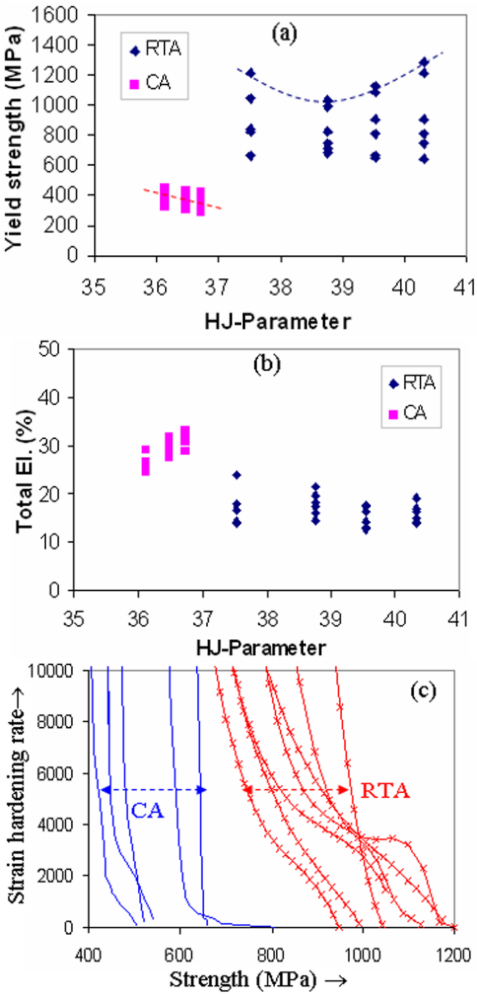


**Figure 4.** Variation in (a) yield strength and (b) total elongation of RTA and CA samples with HJ-parameter. (c) Comparison between the RTA and CA samples in terms of strain-hardening rate

Decrease in strength and increase in elongation of CA samples with the increase in HJ-parameter (Figure 4(a, b))

can be related to the increase in recrystallistallised fraction and coarsening of the θ-particles. Change in the mechanical properties of RTA samples was controlled by a more complex interaction between α-recrystallistaion and austenite (γ) formation. Initial decrease in YS (and also UTS) with the increase in the annealing time to 15 s, as indicated by the dotted lines in Figure 4a can be attributed to the softening of α-grains by recrystallisation. Subsequent rise in strength with further increase in annealing time till 60 s could be dictated by the increase in γ fraction, which contributed to the increased fraction of hard phases (bainite and martensite).

Fine α-grain size (≤ 5 μm) not only contributed to ~350 MPa as grain boundary strengthening but also can ensure decent ductility by activating more number of slip-systems during plastic deformation, compared to the coarser grains. Bimodal α-grain structures with ultra-fine grains (Figure 4e) can also provide an ideal combination of strength and ductility[7]. Hard phases such as, bainite and martensite not only increased the strength, but also improved the strain-hardening ability of RTA samples, with respect to CA samples, Figure 4c, by generating geometrically necessary dislocations in ferritic regions adjacent to the hard-phases [19]. As a result, RTA showed higher yield to tensile strength ratio (0.75 ± 0.08) than that in CA (0.87 ± 0.03), which makes RTA samples a better choice from the formability point of view. Formation of geometrically necessary dislocations in RTA samples also eliminated the yield point phenomenon, which can be in seen in the stress-strain curves of CA samples, Figure 3. If the yield point elongations (4-7%) are not considered, then the amount of homogeneous plastic strain in CA and RTA samples become comparable, Figure 3 and Table 1. Average tensile toughness, represented by the area under the stress-strain curves, for the RTA samples (160 ± 51 MPa) is similar to that for the CA samples (167 ± 65 MPa). Future studies will compare the CA and RTA treated samples in terms of impact toughness and fracture toughness.

In spite of several advantages of the RTA treatment over CA treatment with respect to the microstructure and tensile properties, the industrial applicability of RTA treatment and its effect on flatness and surface quality of cold-rolled sheets remains a challenging task. Although, recent interest on flash processing and rapid annealing provide a ray of hope[14], future research and industrial projects need to concentrate on this aspect.

# 4. Conclusions

In summary, comparative assessment between conventional annealing (CA) and rapid transformation annealing (RTA) treatments on cold-rolled samples of different starting microstructures showed that RTA samples offered higher strength (YS>800 MPa) along with better strain-hardening ability, absence of yield point phenomenon and comparable tensile toughness, with respect to the CA samples (YS<500 MPa). Amongst different starting microstructures, ferrite+fibrous-martensite structure showed the best combination of strength and ductility after RTA.

# ACKNOWLEDGEMENTS

Council of Scientific and Industrial Research (CSIR), New Delhi for the financial support.

# REFERENCES

[1] P. Ghosh, B. Bhattacharya, R. K. Ray: Scripta Met. 56 (2007) 657-660.

[2] S. G. Chowdhury, E. V. Pereloma, D. B. Santos: Mat. Sci. and Eng. A 480 (2008) 540-548.

[3] R. O. Rocha, T. M. F. melo, E. V. Pereloma, D. B. Santos: Mat. Sci. And Engg. A 391 (2005) 296-304.

[4] R. Song, D. Ponge, D. Raabe, J. G. Speer, D. K. Matlock: Mat. Sci. and Eng. A 441 (2006) 1-17.

[5] A. K. Srivastava, D. Bhattacharjee, G. Jha, N. Gope, S. B. Singh: Mat. Sci. And Eng. A 445-446 (2007) 549-557.

[6] R. Ueji, N. Tsuji, Y. Minamino, Y. Koizumi: Acta Materialia 50 (2002) 4177-4189.

[7] H. Azizi-Alizamini, M. Militzer, W. J. Poole: Scripta Mater. 57 (2007) 1065-1068.

[8] S. M. Hasan, A. Haldar, D. Chakrabarti: Mat. Sci. Technol., Accepted paper, (2012), DOI: 10.1179/ 1743284711Y. 0000000113.

[9] C. Lesch, P. Alvarez, W. Bleck, J. Gil Sevillano, Metall. Mater. Trans. 38A (2007) 1882–1890.

[10] P. Alvarez, C. Lesch, W. Bleck, H. Petitgand, J. Schöttler, J. Gil Sevillano, Mater. Sci. Forum 500–501 (2005) 771–778.

[11] V. Massardiera, A. Ngansopa, D. Fabrègue, J. Merlin, Mater. Sci. Eng. A 527 (2010) 5654–5663.

[12] R. A. Grange, Metallurgical transactions. 2 (1971) 65-78.

[13] V. Andrade-Carozzo, P. J. Jacques: Mat. Sci. Forum 539-543 (2007) 4649-4654.

[14] T. Lolla, G. Cola, B.Narayanan, B. Alexandrov, S. S. Babu: Mat. Sci. and Technol. 27 (2011) 863-875.

[15] J. Huang, W. J. Poole, M. Militzer: Metall. Mater. Trans. A, 35 (2004) 3363-3375.

[16] F. G. Caballero, C. Capdevilla, C. Garcia De Andres: ISIJ Int. 43 (2003) 726-735.

[17] K. Hono, M. Ohnuma, M. Murayama, S. Nishida, A. Yoshie and T. Takahashi: Scripta Mater. 44 (2001) 977- 983.

[18] H. Azizi-Alizamini, M. Militzer, W. J. Poole: ISIJ Int. 51 (2011) 958-964.